

# An EPR Study of Two-Electron Sensitization by Fragmentable Donors

*T. D. Pawlik, A. A. Muentzer, R. S. Eachus, and J. R. Lenhard*  
*Eastman Kodak Company*  
*Rochester, New York/USA*

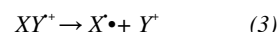
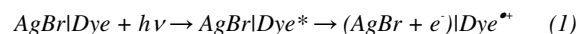
## Abstract

Fragmentable two-electron donors are molecules that have been designed to undergo a bond fragmentation reaction after capturing the hole created by photoexposure of AgX. As part of the design, the radical remaining after fragmentation is made reducing enough so that it can inject an electron into the AgX conduction band. Use of these compounds, thus, allows for the creation of two electrons for each absorbed photon. Photographic results confirm that two-electron sensitization can yield the expected 2X gain in photosensitivity. In this report, electron paramagnetic resonance (EPR) is used to study the mechanism of hole capture, fragmentation, and electron injection. In order to monitor the electron injection, we use a silver halide dispersion doped with a transition metal complex as a deep electron trap. The deep electron trap becomes paramagnetic after electron capture; therefore, EPR can be used to measure the concentration of trapped electrons. In a sample that is exposed at 15 K, the electron injection is observed as an increase in the trapped electron signal upon annealing to the temperature at which fragmentation of the two-electron sensitizer occurs. Self-trapped hole centers and organic radicals associated with the fragmentable donor, or sensitizing dye, are other paramagnetic species that can be monitored by EPR throughout the annealing process. The results confirm the proposed mechanism of hole capture, fragmentation, and electron injection. The reactivities of different two-electron sensitizing materials are reflected in the different onset temperatures of the injection of the second electron.

## Introduction

A method to substantially increase the imaging efficiency of state-of-the-art photographic materials has been reported by Gould et al.<sup>1</sup> and described in several patents.<sup>2-4</sup> This approach is summarized in Scheme 1.

### Scheme 1



The photographic system, described as AgBr|Dye in Eq. 1, consists of silver halide microcrystals (or grains) dispersed in gelatin. These grains are usually spectrally sensitized with an adsorbed dye. The novel aspect of this scheme entails the co-addition of an electron donor molecule, XY. Light absorption by the dye initiates the transfer of an electron to the conduction band of the silver halide substrate,<sup>5</sup> a condition represented here as (AgBr + e). This is the first step in latent image formation.<sup>5</sup> The resultant oxidized dye radical, Dye<sup>••</sup>, reacts with XY to give a radical cation, XY<sup>••</sup>, which fragments to a radical X<sup>•</sup> and a stable cation Y<sup>+</sup>. XY is described as a fragmentable electron donor, or FED. Its structure is designed so X<sup>•</sup> is a powerful reductant and has the potential to transfer a second electron into the silver halide conduction band. Thus two electrons are injected per absorbed photon, effectively doubling the imaging efficiency of the system. This type of FED is referred to as a two-electron sensitizer, or TES.

There is a potential additional advantage to the co-addition of XY and the dye. The reverse of Eq. 1, i.e., recombination of the injected electron with an oxidized dye radical at the grain's surface, can limit the imaging efficiency of the system. In this situation, the rapid reaction of Dye<sup>••</sup> with XY (Eq. 2) should suppress this loss process and, thereby, increase the system's imaging efficiency, even if X<sup>•</sup> is unable to subsequently inject a second electron.

It is also possible for the FED compound to function in the absence of a sensitizing dye. In this case, the photon is absorbed directly as a band-gap excitation of the silver halide, creating an electron and hole. The XY moiety captures the photo hole, and the fragmentation and electron injection steps occur as described above. Photographic measurements on both undyed and dyed silver halide dispersions containing a range of FED molecules have confirmed significant sensitivity increases from the addition of the FED compounds. Solution-transient absorption studies of related model systems have indirectly supported the proposed TES mechanism for this sensitivity increase.<sup>1-4</sup>

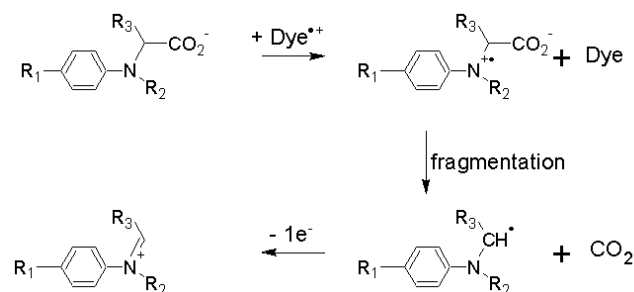
In this report, we present spectroscopic evidence for the two-electron mechanism based upon magnetic resonance measurements on silver bromide dispersions.

## Experimental Strategy

Because the intermediates  $\text{Dye}^{*\bullet}$ ,  $\text{XY}^{*\bullet}$ , and  $\text{X}^{\bullet}$  are paramagnetic, photo-EPR (Electron Paramagnetic Resonance) spectroscopy is an appropriate technique to test Scheme 1. Transient optical absorption data from Ref. 1 suggest that these radicals are likely to be very short lived in photographic dispersions at room temperature. In order to stabilize them sufficiently to facilitate continuous-wave EPR studies, irradiations and measurements have been performed at low temperatures. To minimize recombination and to test for secondary electron injection, the silver bromide grains were doped internally with one of several transition-metal complexes known to function as deep electron traps. The best dopants for this purpose proved to be the diamagnetic anions  $[\text{Cl}_3\text{Rh}(\text{H}_2\text{O})]^{2-}$  and  $[\text{Cl}_3\text{Os}(\text{NO})]^{2-}$ .<sup>6-8</sup> The corresponding  $[\text{Cl}_3\text{Rh}(\text{H}_2\text{O})]^{3+}$  and  $[\text{Cl}_3\text{Os}(\text{NO})]^{3+}$  trapped electron centers are long-lived in AgBr dispersions and their EPR spectra are known. The radical intermediates of interest are formed at, or near to, surfaces of the silver halide grains. Thus, their concentrations should increase with the surface-to-volume ratio of the substrate. For this reason, our experiments have been confined to cubic AgBr grains with small edge lengths, typically  $0.1 \pm 0.01 \mu\text{m}$ .

For a FED molecule to function as a two-electron sensitizer in the silver halide system, three requirements are necessary: the oxidation potential of the parent molecule must be low enough to allow the molecule to capture the photohole created in the silver halide or in the dye; the fragmentation reaction must occur within the time scale of silver halide latent image formation; and the radical created by the fragmentation must be sufficiently reducing to inject an electron into the silver halide conduction band. The XY FED molecules selected for this study were amino acids, which, upon oxidation by a photo hole or by  $\text{Dye}^{*\bullet}$ , are expected to give intermediates that can rapidly fragment by decarboxylation to  $\alpha$ -amino radicals with strongly negative oxidation potentials.<sup>1</sup>

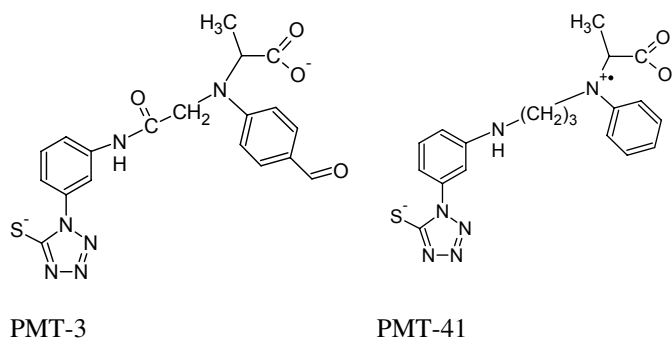
### Scheme 2



In the amino acid structure shown in Scheme 2 above, the oxidation potential of the parent compound can be varied by changing the substituents  $\text{R}_1$  and  $\text{R}_2$ . The fragmentation rate after oxidation is also strongly correlated with this oxidation potential, with compounds having lower oxidation potentials exhibiting slower fragmentation rates. The substituent  $\text{R}_3$  influences the reducing power of the

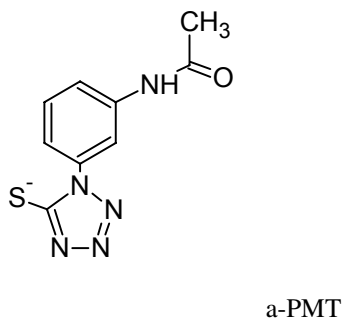
radical remaining after fragmentation. Radicals where  $\text{R}_3$  is methyl have been found to have oxidation potentials more negative than  $-0.9 \text{ V}$ , the condition required for the radical to easily inject an electron into the AgBr conduction band.

A further requirement for the FED compounds to be useful sensitizers is that they should be adsorbed to the silver halide surface. While this can be accomplished by adding high concentrations of the simple amino acid structures to silver halide dispersions, it is preferable to use compounds where a covalent linkage to an adsorbing moiety is provided.<sup>2</sup> Structures for the two FED examples employed in the majority of this work are shown below. In these compounds,  $\text{R}_2$  is a linking bridge to a phenyl mercaptotetrazole, a moiety that is known to adsorb strongly to silver halide by complexation of the mercapto group with silver ion.<sup>9</sup>



In PMT-3, the  $\text{R}_1$  formyl substituent leads to a relatively high oxidation potential for the FED moiety, approximately  $1.14 \text{ V}$ , and a very rapid room temperature fragmentation rate, about  $4 \times 10^{11} \text{ s}^{-1}$ . In PMT-41, with H as  $\text{R}_1$  in the FED moiety, the estimated oxidation potential is lower,  $0.81 \text{ V}$ , and the room temperature fragmentation rate slower, about  $8 \times 10^8 \text{ s}^{-1}$ .<sup>1,10</sup>

The substituted phenyl mercaptotetrazole, a-PMT, was used as the reference addendum for these experiments. This compound is expected to interact with the silver halide surface in a manner similar to PMT-3 or PMT-41 but will not fragment.



### Undyed $\text{Rh}^{3+}$ -doped AgBr

(i) *With no surface addenda.* Figure 1 shows a  $9.3 \text{ GHz}$  EPR spectrum obtained from a dried AgBr dispersion

in which the 0.1  $\mu\text{m}$  cubic grains were doped nominally with 100 molar parts per million of  $[\text{Cl}_5\text{Rh}(\text{H}_2\text{O})]^{2-}$ . The sample was free of dye and FED. This spectrum was measured with the sample at 15 K following its exposure to actinic light at that temperature. The spectrum is presented in the usual first-derivative mode as the solid line, while the dotted curve is its integral. There are features from at least three photo-generated species convoluted in this spectrum. They can be assigned by inspection from a comparison to literature data.

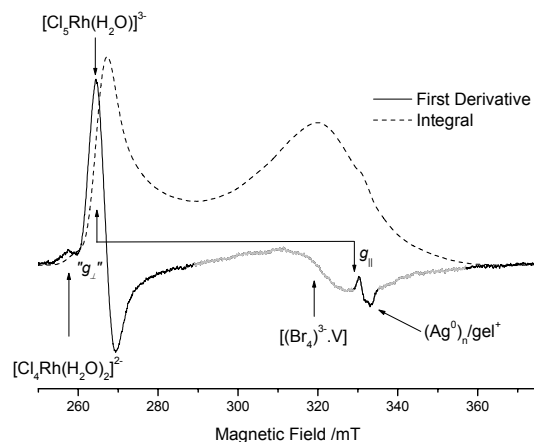


Figure 1. A 9.3 GHz EPR spectrum obtained at 15 K following the exposure of an evaporated AgBr dispersion to actinic light. The AgBr grains were doped with 100 molar ppm of  $[\text{Cl}_5\text{Rh}(\text{H}_2\text{O})]^{2-}$ . The solid line is the usual first-derivative presentation; the dotted line is its integral. The region shaded gray is attributed to  $[(\text{Br}_4)^3 \cdot \text{V}]$  trapped hole centers—see text for details.

The signal shaded gray and centered near to 320 mT is from the intrinsic hole center  $[(\text{Br}_4)^3 \cdot \text{V}]$ .<sup>8</sup> This defect comprises a hole shared by four equivalent bromide ions in a planar array around a silver ion vacancy (V). It is located at, or near to, the grain's surface. The weak, narrower signal near 330 mT results from a small population of silver atom clusters,  $(\text{Ag}^0)_n$ , oxidized gelatin radicals,  $\text{gel}^\dagger$ ; or a mixture of these species.<sup>11</sup> These gelatin radicals, of unspecified composition, are thought to form at the AgBr grain surface when photo holes oxidize the peptizing polymer. The strongest feature in the spectrum is from the trapped electron center  $[\text{Cl}_5\text{Rh}(\text{H}_2\text{O})]^{3-}$ . This complex has orthorhombic or lower symmetry, but  $g_x$  and  $g_y$  differ by less than 0.01; therefore, in X-Band, they are convoluted into the perpendicular-like feature  $g_\perp$  at 264 mT ( $g = 2.5_2$ ). The expected feature corresponding to  $g_\parallel \approx 2.0$  is broad, weak, and obscured by the intrinsic hole signal around 330 mT. The first derivative presentation in Fig. 1 makes it difficult to estimate the relative concentrations of the three photo products. It suggests that the yield of trapped electron centers is substantially greater than that of  $[(\text{Br}_4)^3 \cdot \text{V}]$ , but

the integrated signal shows that they are actually produced in about equal concentrations.

To obtain metrics for the concentrations of  $\text{Rh}^{2+}$  trapped electron centers<sup>†</sup>,  $A_e$ , and  $[(\text{Br}_4)^3 \cdot \text{V}]$ ,  $A_h$ , the first-derivative EPR spectrum in Fig. 1 was doubly integrated. The  $\text{Rh}^{2+}$  signal in the region of “ $g_\perp$ ” is substantially shifted downfield from  $g = 2$ . Thus the area between 250 and 280 mT gives a good measure of  $A_e$ . On the other hand, the high-field region of the spectrum from  $[(\text{Br}_4)^3 \cdot \text{V}]$  strongly overlaps those derived from several organic radicals observed in this study. To obtain a consistent measure of  $A_h$ , we have only used the area under the signal between 300–325 mT.

(ii) With *a*-PMT. The addition of up to 2 mM/M AgBr of the non-fragmenting compound, *a*-PMT, affected the photochemistry of the dispersion. For band-gap exposures at 15 K, the formation of  $\text{Rh}^{2+}$  centers was basically unchanged by the addition of the donor, but the EPR signal from  $[(\text{Br}_4)^3 \cdot \text{V}]$  hole centers was shifted to higher field (lower  $g$  factor). It is possible that this shift in the  $[(\text{Br}_4)^3 \cdot \text{V}]$  spectrum reflects a change in the surface structure of the AgBr grains. *a*-PMT is known to bind strongly to  $\text{Ag}^+$  ions and it suppresses cation interstitial formation at AgBr surfaces.<sup>9</sup>

(iii) With PMT-41.

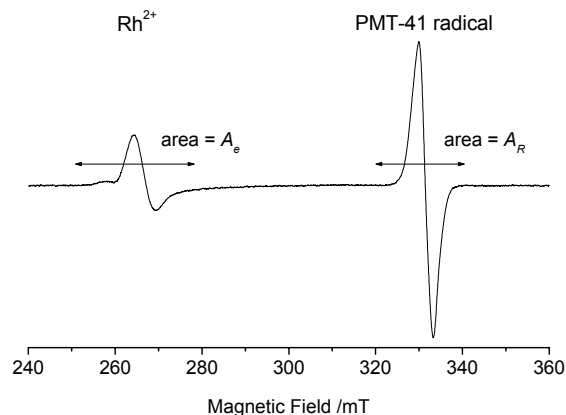


Figure 2. 9.3 GHz EPR spectra obtained at 15 K following the exposure of evaporated AgBr dispersions to 365–440nm light.

The AgBr grains were doped with 100 molar ppm of  $[\text{Cl}_5\text{Rh}(\text{H}_2\text{O})]^{2-}$ . PMT-41 was added at a concentration of 2 mM/M AgBr.

The X-band EPR spectrum in Fig. 2 was obtained at 15 K from an AgBr dispersion in which the 0.1  $\mu\text{m}$  cubic grains were doped nominally with 100 molar ppm of  $[\text{Cl}_5\text{Rh}(\text{H}_2\text{O})]^{2-}$  and to which PMT-41 was added at a concentration of 2.0 mM/M AgBr. The dried dispersion was

<sup>†</sup>  $\text{Rh}^{2+}$  is used here to denote a combination of  $[\text{Cl}_5\text{Rh}(\text{H}_2\text{O})]^{3-}$ ,  $[\text{Cl}_4\text{Rh}(\text{H}_2\text{O})_2]^{2-}$  and  $(\text{RhCl}_4)^+$  trapped electron centers.

exposed to band-gap radiation for 660 s at 15 K. Signals from  $\text{Rh}^{2+}$  trapped electron centers are evident in the region between 250 and 280 mT and an intense single line at about 331.5 mT ( $\Delta B_{p-p} = 3.3$  mT) is observed. This results from a new radical. Formation of the intrinsic hole center  $[(\text{Br}_4)^{3-}\cdot\text{V}]$  is suppressed at this FED concentration, although it was still detected in dispersions treated with  $\leq 0.3$  mM/M AgBr of PMT-41. This suggests that the new signal in Fig. 2 results from a trapped hole center, such as an oxidized PMT-41<sup>•+</sup> radical or its decomposition product.

Annealing the irradiated dispersion for 10 minutes in the dark caused significant changes in the EPR spectrum obtained after quenching back to 15 K. Figure 3 compares annealing data obtained from dispersions with three different concentrations of the FED added. Values for  $A_e$  and  $A_h$  from the sample containing no FED are included for reference as well as  $A_h$  from the sample treated with 0.3 mM/M AgBr of PMT-41. For convenience in separating the two signals in this and subsequent plots, the  $A_R$  and  $A_e$  signals are normalized to 1.0 at 15 K, while the  $A_h$  signal is normalized to 0.5. There was an initial rise in the PMT-41<sup>•+</sup> radical concentration upon annealing to 90 K. This increase was largest for the dispersion with the lowest level of this FED. In this sample,  $A_R$  reached a maximum value at about 120 K, by which temperature any intrinsic hole centers had

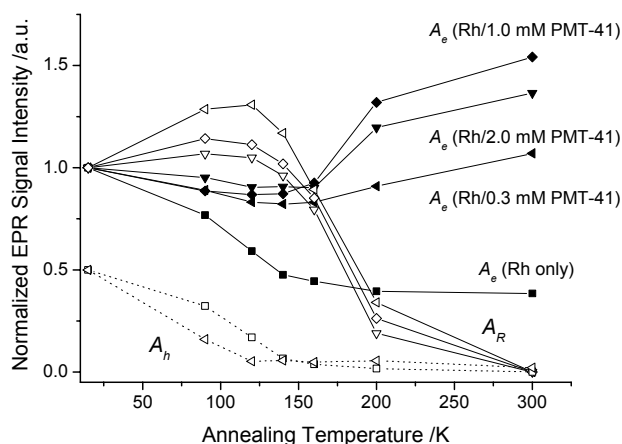


Figure 3. Plots of signal intensity-vs-annealing temperature for four  $[\text{Cl}_3\text{Rh}(\text{H}_2\text{O})]^{2-}$ -doped AgBr dispersions. (i) No surface addenda, (ii) PMT-41 at a concentration of 0.3 mM/M AgBr, (iii) PMT-41 at a concentration of 1.0 mM/M AgBr, and (iv) PMT-41 at a concentration of 2.0 mM/M AgBr.  $A_e$  represents the concentration of  $\text{Rh}^{2+}$  centers,  $A_h$  represents the concentration of  $[(\text{Br}_4)^{3-}\cdot\text{V}]$  hole centers, and  $A_R$  represents the concentration of PMT-41<sup>•+</sup> radicals.

decayed. This correlation indicates that one of the decay pathways for the  $[(\text{Br}_4)^{3-}\cdot\text{V}]$  centers is transfer of the hole to the PMT-41, either directly at the surface or indirectly via the AgBr valence band. The absence of detectable concentrations of  $[(\text{Br}_4)^{3-}\cdot\text{V}]$  centers in the dispersions

treated with higher levels of the FED accounts for the smaller increases in PMT-41<sup>•+</sup> radical concentrations obtained by annealing.

Without the addition of PMT-41, the concentration of  $\text{Rh}^{2+}$  electron traps decreased on annealing until, at 300 K, about 40% of the trapped electron centers survived. The addition of PMT-41 suppressed recombination at the  $\text{Rh}^{2+}$  centers and, at a level of 1 mM/M AgBr, actually produced an increase in  $\text{Rh}^{2+}$  level after annealing above 160 K. At 300 K, the  $\text{Rh}^{2+}$  signals increased to about 150% of their original intensities. This increase in the  $\text{Rh}^{2+}$  signal is accompanied by decay of the PMT-41<sup>•+</sup> radical between 160 and 300 K. This result indicates secondary electron injection into the AgBr substrate by the PMT-41<sup>•+</sup> radical, either directly or via an intermediate decomposition product. A further increase of the PMT-41 level to 2 mM/M did not lead to an additional increase in  $\text{Rh}^{2+}$  signal.

(iv) *With PMT-3.* Similar results to those reported for PMT-41 were obtained for PMT-3. The addition of this fragmentable electron donor at a concentration of 2 mM/M to a  $\text{Rh}^{2+}$ -doped AgBr dispersion suppressed the formation of intrinsic hole centers during band-gap irradiation at 15 K.

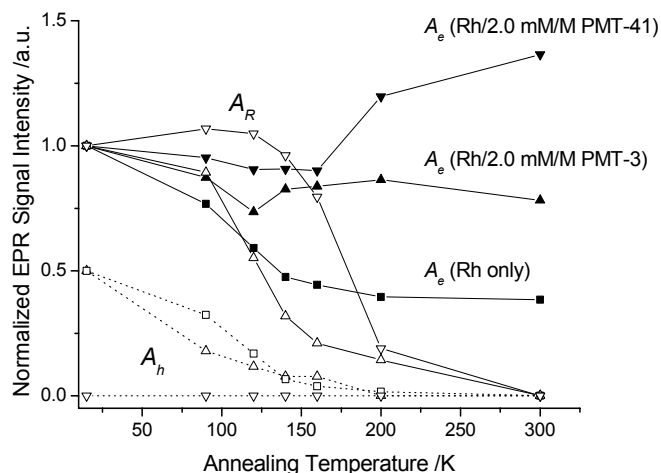


Figure 4. Plots of signal intensity-vs-annealing temperature for three  $[\text{Cl}_3\text{Rh}(\text{H}_2\text{O})]^{2-}$ -doped AgBr dispersions. (i) No surface addenda; (ii) PMT-3 at a concentration of 2.0 mM/M AgBr, and (iii) PMT-41 at a concentration of 2.0 mM/M AgBr.  $A_e$  (closed symbols) represents the concentration of  $\text{Rh}^{2+}$  centers,  $A_h$  (open symbols, dotted lines) represents the concentration of  $[(\text{Br}_4)^{3-}\cdot\text{V}]$  hole centers, and  $A_R$  (open symbols, solid lines) represents the concentration of PMT-3<sup>•+</sup> or PMT-41<sup>•+</sup> radicals.

This suppression, the result of the competitive formation of oxidized FED radicals, was similar to that seen for the 0.3 mM/M level of PMT-41. The appropriate concentration of  $\text{Rh}^{2+}$  trapped electron centers was also produced. The PMT-3 radicals were detected by 9.3 GHz EPR spectroscopy as a single line centered at 331.5 mT

with  $\Delta B_{pp} = 2.6$  mT. The effects of PMT-3 were also evident in annealing experiments. Figure 4 compares data from dispersions treated with no surface addendum, 2.0 mM/M AgBr of PMT-3, and PMT-41 at the same concentration.

Although their effects are similar, PMT-3 is a less efficient hole trap than PMT-41. In addition, PMT-3<sup>•+</sup> is observed to be less stable than PMT-41<sup>•+</sup>, as disappearance of PMT-3<sup>•+</sup> begins at roughly 90 K vs 140 K for PMT-41<sup>•+</sup>. This stability difference is consistent with the known higher rate of fragmentation in RT solution for the PMT-3 oxidized FED moiety.<sup>1,10</sup> As in the case of PMT-41<sup>•+</sup>, the disappearance of the PMT-3<sup>•+</sup> is accompanied by a significant lessening of the loss of the Rh<sup>2+</sup> signal with increasing temperature. These results support the contention that, like PMT-41<sup>•+</sup>, the PMT-3<sup>•+</sup> radical is a source of secondary electrons in AgBr dispersions.

In the course of PMT-3<sup>•+</sup> decomposition, a weak signal from a new radical was observed (see Fig 5), its concentration reaching a maximum value after annealing at 160 K for about 10 min. For annealing temperatures of 200 K and higher, the radical is no longer present. The signal is weak and broad, but it is possible to resolve splittings of about 2 mT in the wings (marked with arrows in the figure). These might be <sup>1</sup>H and/or <sup>14</sup>N hyperfine splittings. Estimates of <sup>1</sup>H hyperfine interactions from *ab-initio* calculations are consistent with this signal originating from the decarboxylated radical.

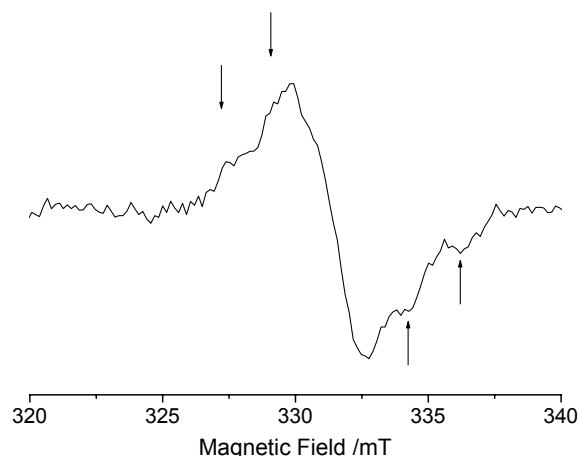


Figure 5. A 9.3 GHz EPR spectrum obtained at 15 K following the exposure of an evaporated AgBr dispersion to 365–440 nm light and annealing in the dark at 160 K for 10 min. Only the central region of the spectrum is shown here. The dispersion was treated with PMT-3 at a concentration of 1.0 mM/M AgBr. The arrows mark potential <sup>1</sup>H and/or <sup>14</sup>N hyperfine features.

#### Dye Sensitized, Rh<sup>3+</sup>-doped AgBr with a-PMT or PMT-3

For any practical application of this technology, the AgBr dispersions will be optically sensitized with an appropriate dye. To assess the effects of adding the FED in combination with a dye, the blue-absorbing, anionic 5-Cl benzothiazole monomethine cyanine dye, B-THC, was added to the system. This molecule readily adsorbs to AgBr grains forming a J- aggregate with peak absorption at about 470 nm. Since its oxidation potential is 1.45 V, it is expected that holes trapped at this dye can transfer to either PMT-3 or PMT-41. The EPR spectrum of a B-THC-sensitized dispersion after light exposure at 15K is qualitatively similar to that of the PMT-41 sensitized dispersion depicted in Fig. 2. The electron injected from the dye into AgX leaves an oxidized dye radical, Dye<sup>•+</sup>. This radical is visible as a single EPR line at 331.5 mT ( $g = 2.0047$ ;  $\Delta B_{pp} = 1.8$  mT). The EPR spectra of Dye<sup>•+</sup> and FED radicals strongly overlap, and deconvolution of these signals, when both were present, was not attempted. Annealing of the sample to 90 K increases the Dye<sup>•+</sup> signal by 20%, while the concentration of the Rh<sup>2+</sup> trapped electron centers is nearly unchanged.

This can be explained by the thermally activated capture of intrinsic holes by the dye, which effectively reduces their recombination with the trapped electron centers (note that in the absence of dye, the Rh<sup>2+</sup> concentration is reduced to 70% at 90 K).

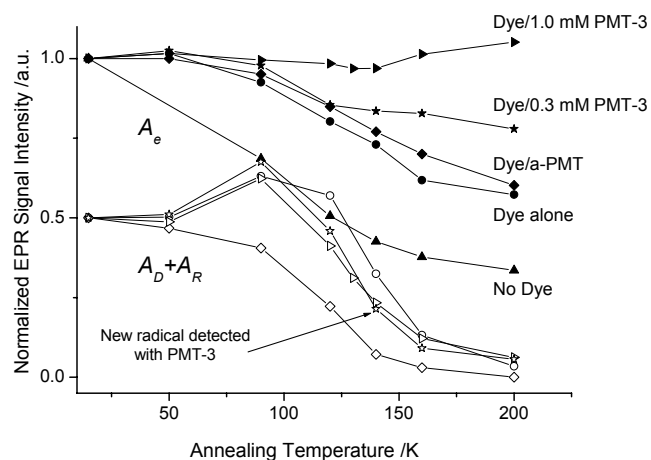


Figure 6. Plots of signal intensity-vs-annealing temperature for five Rh<sup>3+</sup>-doped AgBr dispersions. (i) No surface addenda; (ii) Dye only; (iii) Dye and a-PMT; (iv) Dye and 0.3 mM/M AgBr of PMT-3; and (v) Dye and 1.0 mM/M AgBr of PMT-3.  $A_D + A_R$  represents the cumulative concentration of Dye<sup>•+</sup> and PMT-3<sup>•+</sup> radicals (open symbols) and  $A_e$  represents the concentration of Rh<sup>2+</sup> trapped electron centers (closed symbols)

Co-addition of a-PMT and dye does not affect the Rh<sup>2+</sup> concentration in this temperature range, but it eliminates the increase in Dye<sup>•+</sup> signal at 90 K. In the undyed, a-PMT-sensitized dispersion, we have observed a modified [(Br<sub>4</sub>)<sup>3-</sup>

.V] hole center. We propose that in the dyed dispersions this hole center competes with the formation of  $\text{Dye}^{\bullet+}$ .

When PMT-3 was added to the dye, the most significant change was observed between 100 and 200 K, where the presence of PMT-3 increased the number of trapped electron centers produced by annealing, compared to situations with dye alone or in combination with a-PMT. This effect, which increased with the concentration of PMT-3 added to the dispersion, is attributed to secondary electron injection into AgBr in a manner similar to that observed for PMT-3 on the undyed AgBr dispersions (Figs. 3 and 4). In these dyed dispersions, it was again possible to observe the radical attributed to the decarboxylated PMT-3 $^{\bullet+}$ . Both of these observations indicate that whether the photo hole is initially created in the AgBr valence band or in a sensitizing dye, the TES process is capable of injecting secondary electrons into the AgBr conduction band.

### Conclusion

The EPR data presented in this report supports the assumption that the proposed TES mechanism, previously verified in solution, takes place at the AgX surface and provides extra electrons in the conduction band of AgX.

For PMT-41, we observe very strong hole trapping by the FED moiety and an actual increase of the number of electrons at Rh centers, as the dispersion is annealed to room temperature. For PMT-3, we also see strong hole trapping and suppression of the loss of  $\text{Rh}^{2+}$  centers as the dispersion is annealed to room temperature. For PMT-3, the radical becomes unstable at a significantly lower temperature than for PMT-41, in agreement with its much faster estimated room temperature fragmentation rate. The lower temperature of fragmentation allows the observation of the decarboxylated radical by EPR.

Experiments with PMT-3 and a blue-absorbing cyanine dye show that the TES mechanism also operates as predicted in the presence of a sensitizing dye.

The presence of a-PMT stabilizes a modified  $[(\text{Br}_2)^3 \cdot \text{V}]$  hole center. This has an effect on the concentration of  $\text{Dye}^{\bullet+}$  hole centers. Consistent with a-PMT's inability to fragment and inject electrons, we observed no increases in the

trapped electron concentration in a-PMT sensitized dispersions.

### References

1. I. R. Gould, J. R. Lenhard, A. A. Muentner, S. A. Godleski, and S. Y. Farid, *J. Am. Chem. Soc.*, **122**, 11934 (2000).
2. S. Y. Farid, J. R. Lenhard, C. H. Chen, A. A. Muentner, I. R. Gould, S. A. Godleski, and P. A. Zielinski, U.S. Patent 5,747,235, (1998).
3. S. Y. Farid, J. R. Lenhard, C. H. Chen, A. A. Muentner, I. R. Gould, S. A. Godleski, P. A. Zielinski, and C. H. Weidner, U.S. Patent 5,747,236, (1998).
4. S. Y. Farid, J. R. Lenhard, C. H. Chen, A. A. Muentner, I. R. Gould, S. A. Godleski, P. A. Zielinski, and C. H. Weidner U.S. Patent 5,994,051, (1999).
5. W. West, P. B. Gilman in *The Theory of the Photographic Process, 4th ed.*; T. H. James, Ed., MacMillan, New York, 1977, pg. 251.
6. T. D. Pawlik, R. S. Eachus, W. G. McDugle, and R. C. Baetzold, *J. Phys.: Condens. Matter*, **10**, 11795, (1998).
7. R. S. Eachus, R. C. Baetzold, T. D. Pawlik, O. G. Poluektov, and J. Schmidt, *Phys. Rev. B*, **59**, 8560 (1999).
8. R. S. Eachus, T. D. Pawlik, and R. C. Baetzold, *J. Phys.: Condens. Matter* **12**, 8893 (2000).
9. T. Tani, *Photographic Sensitivity: Theory and Mechanisms*, Oxford University Press, New York, Chapter 6, 1995, pg. 185–186.
10. I. R. Gould and S. Y. Farid, private communication
11. T. D. Pawlik, R. S. Eachus, R. C. Baetzold and W. G. McDugle, *J. Phys.: Condens. Matter*, **12**, 2555 (2000).

### Biography

Thomas Pawlik is a Senior Research Scientist in the Imaging Materials Division of the Eastman Kodak Company Research & Development Laboratories. He received his PhD in solid-state physics from the University of Paderborn, Germany in 1996. His research interests include the photophysics of silver halide imaging materials and charge transport and recombination in organic semiconductors.